

# Random degree-degree correlated networks

Marlon Ramos<sup>1</sup> and Celia Anteneodo<sup>1,2</sup>

<sup>1</sup> *Department of Physics, PUC-Rio, Rio de Janeiro, Brazil*

<sup>2</sup> *National Institute of Science and Technology for Complex Systems, Rio de Janeiro, Brazil.*

(Dated: April 23, 2019)

Correlations may affect propagation processes on complex networks. To analyze their effect, it is useful to build ensembles of networks constrained to have a given value of a structural measure, such as the degree-degree correlation  $r$ , being random in other aspects and preserving the degree distribution. This can be done through Monte Carlo optimization procedures. Meanwhile, when tuning  $r$ , other network properties may concomitantly change. Then, in this work we analyze, for the  $r$ -ensembles, the impact of  $r$  on properties such as transitivity, branching and characteristic lengths, that are relevant when investigating spreading phenomena on these networks. The present analysis is performed for networks with degree distributions of two main types: either localized around a typical degree (with exponentially bounded asymptotic decay) or broadly distributed (with power-law decay). Correlation bounds and size effects are also investigated.

PACS numbers: 64.60.aq, 64.60.an, 05.40.-a

## I. INTRODUCTION

Complex networks are realistic substrates for simulating many social and natural phenomena. To address the influence of network topology, primarily, different classes of degree distributions  $P(k)$  can be considered. Meanwhile, for a given distribution of degrees, correlations may give rise to important network structure effects on the studied process [1–5], for instance shifting the epidemic threshold [5]. Hence correlations can not be neglected. However, joint probabilities of two or more degrees measured in networks of moderate size may be noisy and hard to model. Then, operationally, average nearest-neighbors degree distributions [6] or single quantity measures are used. Although other variants have been defined in the literature [7, 8], as quantifier of the tendency of adjacent vertices to have similar or dissimilar degrees, we will consider the standard measure of (linear) degree-degree correlations, namely, the assortativity (Pearson) coefficient

$$r = \frac{\langle kk' \rangle_e - \langle k \rangle_e^2}{\langle k^2 \rangle_e - \langle k \rangle_e^2}, \quad (1)$$

where  $\langle \dots \rangle_e$  denotes average over edges and  $k$  and  $k'$  are the degrees of vertices at each end of an edge.

To analyze the influence of correlations, as well as of any other structural feature, it is useful to build ensembles of networks holding that property, while keeping fixed the distribution of degrees. As it will be described in Sec. II, this kind of ensembles can be achieved by means of a suitable rewiring that does not affect the degree distribution, performed through a standard simulated annealing Monte Carlo (MC) procedure to minimize a given energy-like quantity (maximum entropy ensemble approach), function of the graph property to be controlled ( $r$  in our case) [9–11]. Once tuned  $r$ , it is important to characterize how other network properties are altered as by product. Some interdependencies among certain network properties have already been shown in

the literature, for real as well as for artificial graphs [10]. Analytical relations have also been derived [12]. In this work, because of the importance in spreading phenomena [13], we will focus on the effect of  $r$  over typical distance measures as well as on the branching and transitivity of links.

As a measure of the average separation between nodes, we consider the average path length  $L$

$$L = \frac{\sum_{i=1}^n \langle L_i \rangle N_i (N_i - 1)}{\sum_{i=1}^n N_i (N_i - 1)}, \quad (2)$$

where  $n$  is the number of (disconnected) clusters and  $N_i$  is the number of nodes in cluster  $i$ . Moreover, being  $d_{kj}$  the distance (number of edges along the shortest path) between nodes  $k$  and  $j$  (taking  $d_{kj} = 0$  if the nodes do not belong to the same cluster), then

$$\langle L_i \rangle = \frac{\sum_{j,k=1}^{N_i} d_{kj}}{N_i (N_i - 1)}. \quad (3)$$

Alternatively, in order to avoid the issue of the divergence of the distance between disconnected nodes, we consider the inverse,  $1/E$ , of the so-called efficiency [14]

$$E = \frac{1}{N(N-1)} \sum_{\substack{1 \leq i, j \leq N \\ i \neq j}} \frac{1}{d_{ij}}, \quad (4)$$

where  $N$  is the number of nodes. It represents a harmonic mean instead of the arithmetic one. We also compute the diameter  $D = \max\{d_{ij}\}$ .

The transitivity of links can be measured by the clustering coefficient

$$C = \frac{6n_{\Delta}}{\sum_{i=1}^N k_i (k_i - 1)}, \quad (5)$$

where  $n_{\Delta}$  is the number of triangles and  $k_i$  is the degree of node  $i$ . Other measures that arise in the decomposition of  $r$  [12] will also be considered.

Besides detecting interdependencies among structural properties, it is also important to know how these properties depend on the system size  $N$ . We will analyze these issues for two main classes of degree distributions (Poisson and power-law tailed). We will also investigate real networks degree sequences.

## II. NETWORKS AND ENSEMBLES

For each class of network, we will consider different values of the size,  $N$ , and the mean degree,  $\langle k \rangle$ , within realistic ranges.

As a paradigm of the class of networks with a peaked distribution of degrees, with all its moments finite, we consider the random network of Erdős and Rényi [15]. Within this model, a network with  $N$  nodes is assembled by selecting  $M$  different pairs of nodes at random and linking each pair. The resulting distribution of links is the Poisson distribution  $P(k) = e^{-\langle k \rangle} \langle k \rangle^k / k!$ , where the mean degree is  $\langle k \rangle = 2M/N$ .

We also analyze networks of the power-law type, i.e., with  $P(k) \sim k^{-\gamma}$ ,  $\gamma > 2$ , corresponding to a wide distribution of degrees, with power-law tails. Then, moments of order  $n \geq \gamma - 1$  are divergent. We built power-law networks by means of the configuration model [16]. Following this procedure, one starts by choosing  $N$  random numbers  $k$ , drawn from the degree distribution  $P(k)$ . They represent the number of edges coming out from each node, where these edges have one end attached to the node and another still open. Second, two open ends are randomly chosen and connected such that, although multiple connections are not forbidden, self connections are not allowed. This second stage is repeated until each node attains the connectivity attributed in the first step. If eventually an edge has an open end, then

it is discarded. However, for large networks, the fraction of discarded edges is negligible [17]. To draw the set of numbers  $k$  with probability  $P(k) = \mathcal{N}k^{-\gamma}$ , with  $k_{min} \leq k \leq k_{max}$  (hence the normalization factor is  $\mathcal{N} = 1 / \sum_{k_{min}}^{k_{max}} k^{-\gamma}$ ), we used the inverse transform algorithm [18]. Notice that the cut-off is  $k_{max} \leq N - 1$  and  $k_{max} \gg k_{min}$ , then we determined  $k_{min}$  to fit the selected value of  $\langle k \rangle$  (within a tolerance of at most 1%), such that

$$\langle k \rangle = \frac{\sum_{k_{min}}^{k_{max}} k^{-\gamma+1}}{\sum_{k_{min}}^{k_{max}} k^{-\gamma}} \simeq \frac{\gamma - 1}{\gamma - 2} \frac{k_{max}^{2-\gamma} - k_{min}^{2-\gamma}}{k_{max}^{1-\gamma} - k_{min}^{1-\gamma}}. \quad (6)$$

Typical histograms for the Poisson and power-law networks are depicted in Fig. 1.

In order to attain a desired value of  $r$ , we follow an standard rewiring approach. We want to build an ensemble of networks  $\{G\}$  with a given value of  $r$  ( $r$ -ensemble) but that are random in other aspects, i.e., making the fewer number of assumptions as possible about the distribution  $P(G)$ . Then, we use an exponential random graph model, such that the set of networks  $\{G\}$  has distribution  $P(G) \propto e^{-H(G)}$ , where  $H(G)$  is a Hamiltonian or energy-like quantity [9]. In order to get an  $r$ -ensemble, with  $r = r_*$ , we consider [10]

$$H(G) = \beta |r - r_*|, \quad (7)$$

where  $\beta$  is a real parameter. The ensemble can be simulated by means of a MC procedure: at each step, a rewiring attempt is accepted with probability  $\min\{1, e^{-[H(G') - H(G)]}\}$ . rewiring steps are performed by randomly selecting two edges that connect the vertices  $a, b$  and  $c, d$ , respectively, and substituting those two links by new ones connecting  $a, c$  and  $b, d$  [19]. Movements yielding double links are forbidden. Notice that this process preserves the connectivity of each node. We start the simulation by taking  $\beta = 0$  [during at most 100 MC steps (MCS), where each MCS corresponds to  $N$  attempts]. The effect of this stage is basically to destroy multiple edges. Subsequently,  $\beta$  is increased (in increments  $\Delta\beta = 1000$ ), at each 50 MCS, until  $r$  stabilizes, typically attaining the prescribed value  $r_*$ .

We checked that the choice of other expressions for  $H(G)$ , vanishing at  $r_*$ , did not affect the results but just the convergence time. Average and standard error of the analyzed quantities were computed once stationarity in the rewiring process was attained, over 64 samples obtained from 8 different realizations of each network at 8 time instants (every 20 Monte Carlo steps).

## III. RESULTS

Let us start by reporting the effects of  $r$  on the clustering coefficient  $C$ .

For the Poisson case, we depict in Fig. 2(a) the behavior of  $C$  as a function of  $r$  for a fixed number of nodes

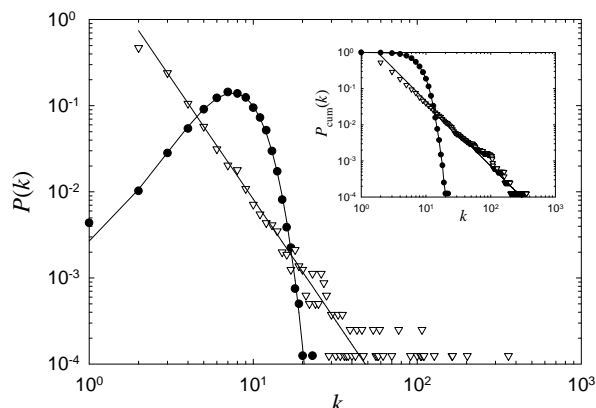


FIG. 1: Degree distribution  $P(k)$  for Poisson (filled symbols) and power-law with  $\gamma = 2.8$  (open symbols) networks, with  $N = 8000$  and  $\langle k \rangle = 4$ . Solid lines join theoretical values. The inset shows the corresponding complementary cumulative distributions.

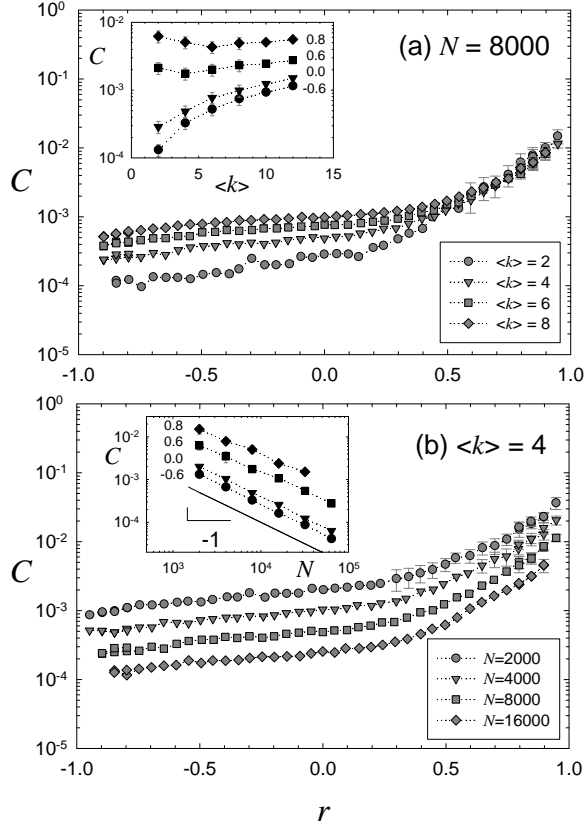


FIG. 2: Clustering coefficient  $C$  as a function of  $r$  for Poisson networks: (a)  $N = 8000$  and different values of  $\langle k \rangle$  indicated on the figure and (b)  $\langle k \rangle = 4$  and different number of nodes  $N$ , also indicated on the figure. Dotted lines are a guide to the eyes. The insets show  $C$  vs  $\langle k \rangle$  (a) and  $N$  (b) for selected values of  $r$  (-0.6, 0.0, 0.6 and 0.8).

( $N = 8000$ ) and different values of the mean connectivity  $\langle k \rangle$ . Very small values of  $C$  emerge. The transitivity  $C$  monotonically increases with  $r$ . This is consistent with the results of Ref. [10] (restricted to  $r \geq 0$ ) for such kind of networks. We observe two regimes with a crossover at  $r \simeq 0.5$ : a very slight increase with  $r$  below the crossover and a more pronounced one in the region above it. Below the crossover,  $C$  rapidly increases with  $\langle k \rangle$  for small values of  $\langle k \rangle$  but slowly, tending to saturate, for large ones. Meanwhile, above the crossover,  $C$  is almost insensitive to changes in the average connectivity already for small  $\langle k \rangle$  (also see the inset of Fig. 2(a) where  $C$  is plotted vs  $\langle k \rangle$  for selected values of  $r$ ). In Sec. IV, we will discuss these issues in more detail.

In Fig. 2(b), size effects are exhibited for  $\langle k \rangle = 4$ , representative of the other values considered. As the number of nodes increases,  $C$  decays as  $C \sim 1/N$  for all  $r$  (as depicted in the inset). Therefore, in the  $r$ -ensemble of Poisson networks, transitivity is only a finite-size effect and vanishes in the infinite network (thermodynamic) limit. Notice that the asymptotic behavior  $C \sim 1/N$  is the natural one for a random graph [25].

For the power-law class, the range of allowed values of  $r$  is restricted. That is, values of  $r$  arbitrarily different from zero can not be attained in typical realizations of the MC protocol described in Sec. II. In order to determine the typical maximal (minimal) values,  $r_{max}$  ( $r_{min}$ ), we imposed  $r_* = 1$  (-1) and detected the stationary values of  $r$ . The time evolution of  $r$  for  $r_* = 1$  (-1) is illustrated in Fig. 3(a) for  $\gamma = 3.5$ ,  $N = 5000$  and  $\langle k \rangle \simeq 4$ . Notice the large deviations amongst the steady values of different realizations mainly for the upper bound. We verified that this picture does not change by implementing other definitions of  $H(G)$  in Eq. (7), e.g.,  $\beta|r - r_*|^\alpha$ , with  $\alpha \neq 1$ . Average extreme values are displayed in Fig. 3(b), as a function of the system size, for different values of  $\gamma$ . For fixed size, the lower  $\gamma$ , the narrower the

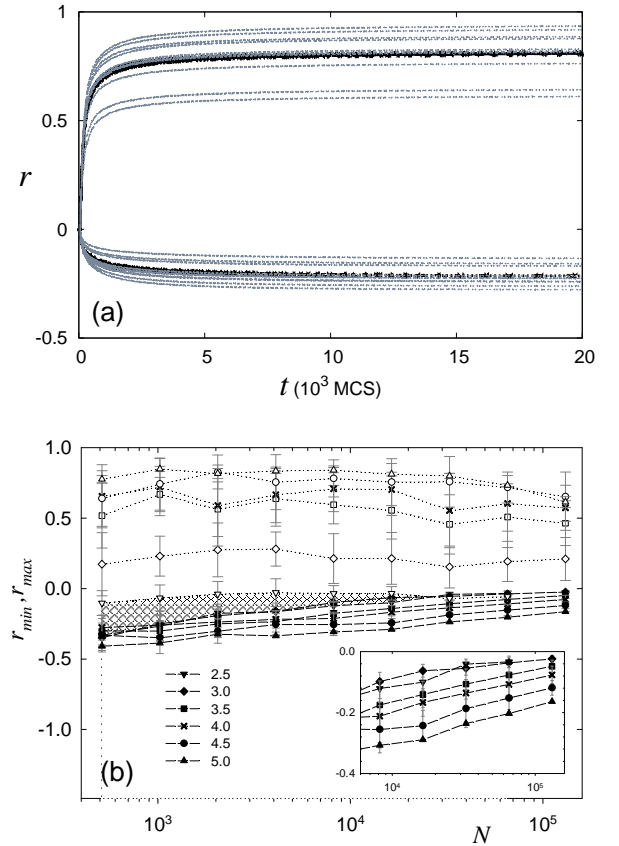


FIG. 3: (a) Time evolution of  $r$ , after setting  $r_* = 1$  (-1) to obtain  $r_{max}$  ( $r_{min}$ ), for networks with power-law degree distribution (with  $\gamma = 3.5$  and  $N = 5000$ ). Shown are 10 individual samples (thin lines) and their respective averages (thick lines). (b) Average extreme values [ $r_{max}$  (open symbols) and  $r_{min}$  (filled symbols) and their standard errors indicated by error bars] vs system size  $N$  for different values of  $\gamma$  indicated on the figure. Dotted and dashed lines are guides to the eye for  $r_{max}$  and  $r_{min}$ , respectively. The shadowed region corresponds to the allowed interval for  $\gamma = 2.5$ , to punctuate the collapse of the interval. The inset is a zoom of the main graph. In all cases  $\langle k \rangle = 4.00 \pm 0.04$ .

allowed interval of  $r$ . For fixed  $\gamma$ , the interval shrinks with system size. In Ref. [6], similar restriction was also observed for  $2 < \gamma < 3$ , although instead of the average connectivity,  $k_{min}$  was kept constant ( $k_{min} = 6$ ). In that case, it was reported that the upper and lower bounds both tend to zero, hence  $r \rightarrow 0$  in the infinite network limit. In fact, we observe that in that interval of  $\gamma$  (e.g.,  $\gamma = 2.5$ ) both bounds are negative and as  $N$  increases the allowed interval collapses to a negative value that tends to zero. We noticed restriction in the correlation bounds for  $\gamma > 3$  too. As  $N$  grows, the lower bound also increases towards zero or at least to a small finite value (see inset of Fig. 3(b)). Simultaneously, the upper bound seems more stable, however its asymptotic behavior is not neat yet, even having considered up to  $N > 10^5$ .

Since the allowed interval of  $r$  is quite restricted for scale-free networks, we analyzed systematically cases with  $\gamma > 3$  ( $\gamma = 3.5, 4.0$  and  $4.5$ ), yielding finite second moment. Even, in this range, the correlation bonds are limited, then, we proceeded as follows. If the desired  $r_*$  is not attained, within a tolerance of  $10^{-3}$ , in  $2 \times 10^4$  MCS, that instance is discarded and we make a new trial. After 10 frustrated trials, we pass to the next value of  $r_*$ . Alternatively to the configuration model, we also started from networks generated by preferential attachment [20], yielding similar results.

The outcomes for the power-law class with  $\gamma = 4.0$  are displayed in Fig. 4. Noisier plots in the power-law case are likely due to the variability in the tails of the distribution of links from sample to sample. Outcomes for the other two values of  $\gamma$  studied (3.5 and 4.5) display features similar to those of the case  $\gamma = 4.0$  used as illustrative example, despite the third moment becoming divergent at  $\gamma = 4.0$ . But some qualitative differences appear in comparison to the Poisson case. Two regimes are also observed, with the crossover now closer to  $r = 0$ .  $C$  rapidly increases with  $r$ , attaining, for assortative networks, larger values than in the Poisson class. This is due to the inclusion of highly connected nodes, absent in the Poisson networks, that for large  $r_*$  tend to gain links among them, contributing strongly to  $r$  and also to  $C$ .

With respect to finite size effects, below the crossover the small non-null  $C$  is again due only to the finite size of the network. However, in the assortative region (above the crossover), it seems that a finite degree of clustering persists for large networks (see inset of 4(b)), in contrast to the Poisson case and to the disassortative region. We will discuss these issues further in Sec. IV.

Let us analyze now the influence of  $r$  on network characteristic lengths. The dependency of the measures  $1/E$ ,  $L$  and  $D$  on  $r$  is depicted in Fig. 5 for  $N = 8000$ ,  $\langle k \rangle \simeq 4$  for Poisson and power-law distributed networks.  $1/E$  and  $L$  have close values, systematically shifted. In first approximation both types of network yield similar values of  $1/E$  (hence also  $L$ ), given  $N$  and  $\langle k \rangle$ . However, the diameter  $D$  is more dependent on the type of network. It is larger and is more strongly affected by  $r$  in the homogeneous Poisson case.

Plots of  $1/E$  vs  $r$  for different values of  $N$  and  $\langle k \rangle$  are shown in Figs. 6 and 7 for Poisson and power-law networks respectively. In both cases, the networks display the small-world property [21] (even smaller in the power-law case) with a slow (logarithmic) increase with  $N$  and a smooth decrease with  $\langle k \rangle$  (see insets of Figs. 6 and 7).

In the Poisson case, the mean path does not depend on  $r$  significantly when  $\langle k \rangle$  is not too small ( $\geq 6$ ), as indicated by the relatively flat plots in Fig. 6(a). Only for small  $\langle k \rangle$  there are important effects for assortative correlations. For instance, for  $\langle k \rangle \simeq 4$  (Fig. 6(b)),  $1/E$  increases in about two units from  $r \simeq 0$  to  $r \simeq 1$ , for all the analyzed sizes. This effect is still larger for  $\langle k \rangle = 2$  where  $L$  increases by a factor about two in the same interval of  $r$ , as shown in Fig. 6(a) for  $N = 8000$ .

In order to further interpret these results, we investigated the cluster structure of the resulting rewired networks. We measured the size of the largest cluster (let us call it  $N_1$ ), the number  $n$  of clusters, and the average size  $S$  of the clusters different from the largest one. The plots are presented in Fig. 8 for  $\langle k \rangle = 2$  and 4. For  $\langle k \rangle = 4$ , the relative size of the largest cluster (circles) is about 0.98 for most of the range of  $r$ , notice however that it slightly decays towards  $|r| = 1$  (which is more evident

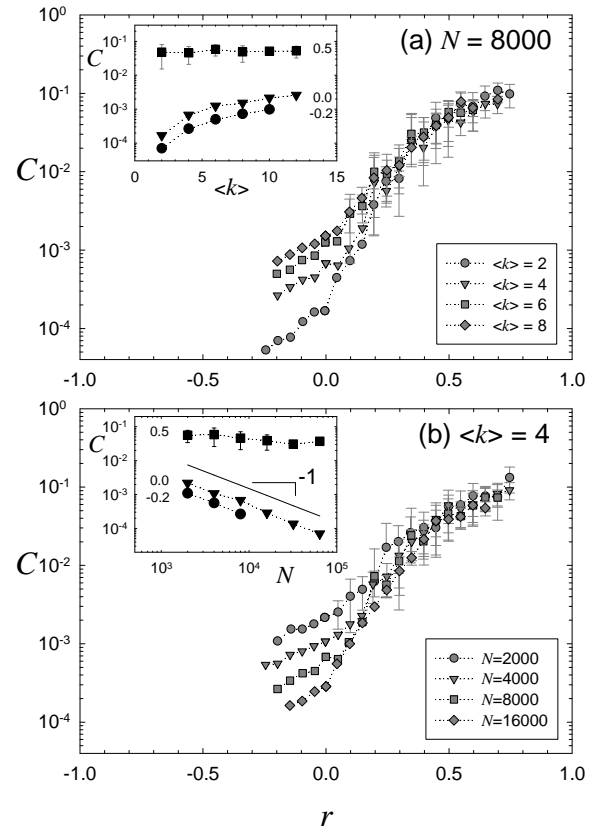


FIG. 4: Clustering coefficient  $C$  as a function of  $r$ , as in Fig. 2 but for power-law networks with  $\gamma = 4.0$ . In the inset, missing values are due to the limitation in attaining the prescribed values of  $r$ .

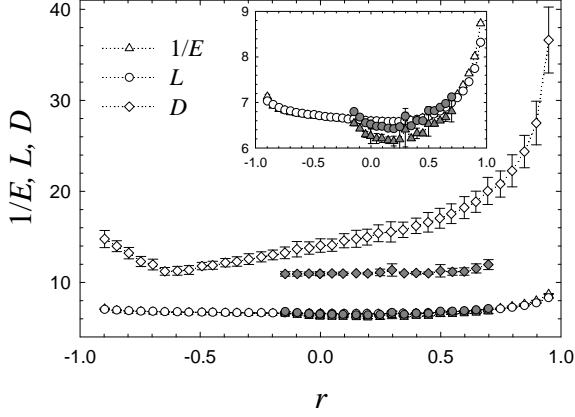


FIG. 5: Distance measures  $1/E$ ,  $L$  and diameter  $D$ , as a function of  $r$  for Poisson (white symbols) and  $\gamma = 4.0$  power-law (gray symbols) networks. In all cases  $N = 8000$  and  $\langle k \rangle = 4.00 \pm 0.04$ . The inset is a zoom of the main plot.

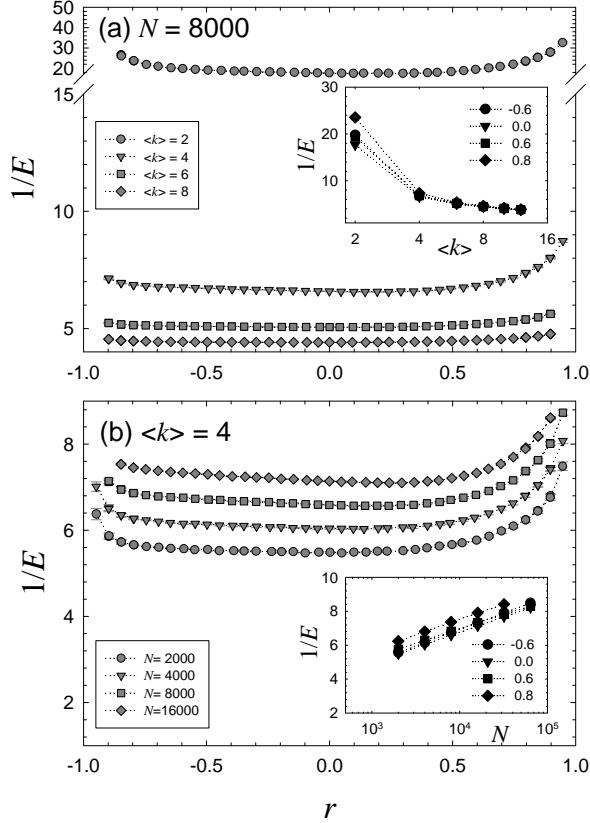


FIG. 6: Mean distance  $1/E$  as a function of  $r$  for Poisson networks: (a)  $N = 8000$  and different values of  $\langle k \rangle$  indicated on the figure and (b)  $\langle k \rangle = 4.00 \pm 0.04$  and different number of nodes  $N$  indicated on the figure.

for  $\langle k \rangle = 2$ . As  $\langle k \rangle$  increases, the number of fragments rapidly decays and the average size  $S$  (triangles) tends to unit, meaning that only single nodes are disconnected

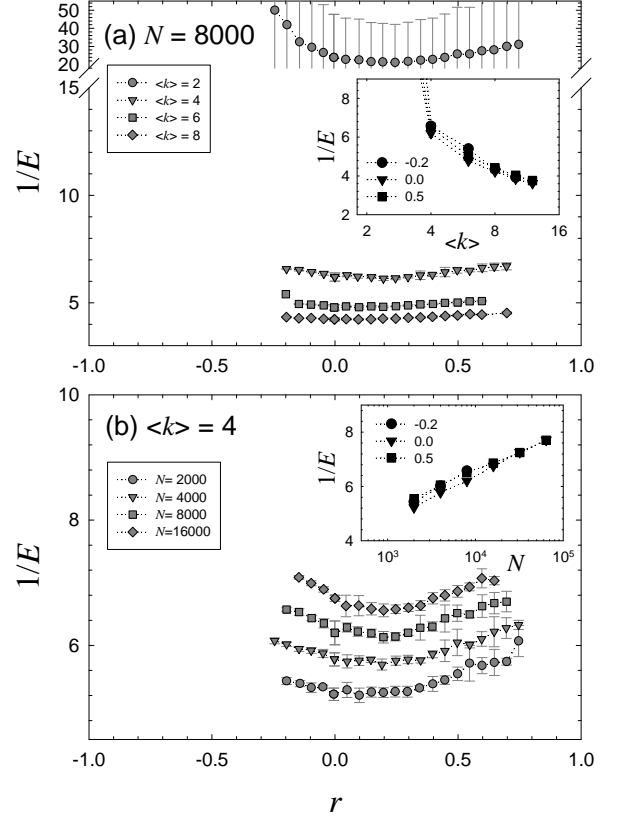


FIG. 7: Mean distance  $1/E$  as a function of  $r$  as in Fig. 6 but for power-law network with  $\gamma = 4.0$ .

(recall also that  $P(0) = e^{-\langle k \rangle}$ ). Therefore the increase

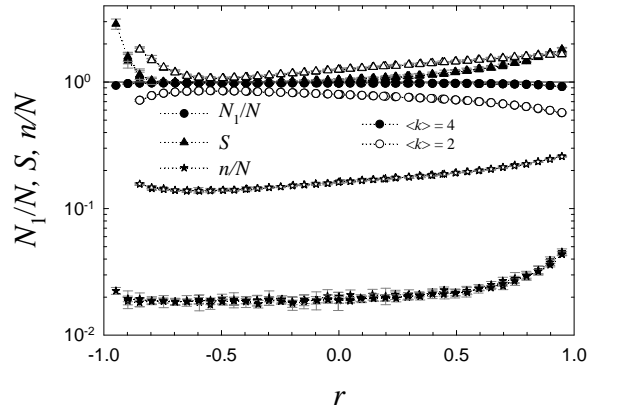


FIG. 8: Clusters analysis. Plots of  $N_1/N$  (where  $N_1$  is the size of the largest cluster) [circles], average size of finite size clusters,  $S$  [triangles], and number of clusters,  $n$  [stars], as a function of  $r$  for Poisson networks with  $\langle k \rangle = 2$  (white symbols) and 4 (filled symbols). Outcomes for different sizes ( $N = 4000, 8000$  and  $16000$ ) all collapse into single curves.

of the mean distance towards  $|r| = 1$ , observed for low  $\langle k \rangle$  in Fig. 6, may simply reflect the fragmentation of the network. Meanwhile, for larger values of  $\langle k \rangle$ , for which the fraction of vertices that do not belong to the largest cluster becomes negligible, the mean distance remains invariant under changes of  $r$ . Hence, transport processes modeled in these networks may suffer important impact when changing  $r$ . The longer the typical separation between nodes, the slower the propagation.

In power-law networks, for fixed  $N$  and  $\langle k \rangle > 2$ , there is an interval of  $r$  where paths are shorter than in the Poisson nets (Fig. 5), and still shorter as  $\gamma$  decreases (not shown). Moreover  $1/E$  becomes more sensitive to the coefficient  $r$  (smile shape), in the region where plots are flat for Poisson networks. Notice also that minimal mean paths occur for slightly assortative correlations ( $r \gtrsim 0$ ), slowly increasing with  $N$  (Fig. 7(b)). The analysis of clusters for  $\gamma = 4.0$ , shows that for  $\langle k \rangle \geq 4$  there is a single cluster of size  $N$ , for all  $r$ . Only for  $\langle k \rangle = 2.0$  we observed fragmentation with  $N_1/N \simeq 0.7 - 0.8$ ,  $n/N \simeq 0.06$ ,  $S \simeq 4$  for all  $N > 2000$  (plots not shown).

For the mean path  $L$ , we observed qualitatively similar outcomes although shifted to slightly higher values, as illustrated in Fig. 5.

We also applied the rewiring procedure described in Sec. II to real degree sequences. Networks were symmetrized and edge weights were ignored. In Fig. 9 we depict the behavior of  $C$  and  $1/E$  vs  $r$ , for the PGP (encrypted communication network using Pretty Good Privacy encryption algorithm) largest component [22], P2P (Gnutella peer-to-peer network) [23], PGR (electrical power grid of the western United States), example of small-world network [24] and APC (astrophysics collaboration network) [25]. First notice that in all cases the clustering  $C$  is much larger in real networks than in the randomized ( $r$ -ensemble) ones, as already observed for other examples in Ref. [10]. The mean distance is also typically larger in the real networks. An exception is P2P network, characterized by a value of  $1/E$  typical of the  $r$ -ensemble. Rewired real networks display some of the typical behaviors observed for the artificial cases. Let us make some remarks arising from comparisons. (i) PGR (power grid) displays plots of  $C$  vs  $r$  and  $1/E$  vs  $r$  that are in good accord with those observed for similar parameters  $\langle k \rangle$  and  $N$  of the Poisson case. In fact its degree distribution decays exponentially. (ii) P2P presents power-law decay of the degree distributions, for  $k > 10$ , with exponent close to  $\gamma = 4$ . Both plots of P2P are in agreement with those obtained for the  $\gamma = 4$  class with similar values of  $N$  and  $\langle k \rangle$ , despite the distributions only share in common the power-law tail. (iii) PGP (of size similar to P2P) has a degree distribution that decays with exponent  $\gamma < 3$  for  $k < 50$  and  $\gamma \simeq 4$  beyond [22]. The plot for  $1/E$  vs  $r$  presents larger values of  $1/E$  than P2P consistent with its  $\langle k \rangle$ . However, the plot  $C$  vs  $r$  of PGP deviates from the standard behavior, presenting larger values of  $C$  that increase with  $r$  in a single regime. The interval of allowed values of  $r$  is sensitive too to details

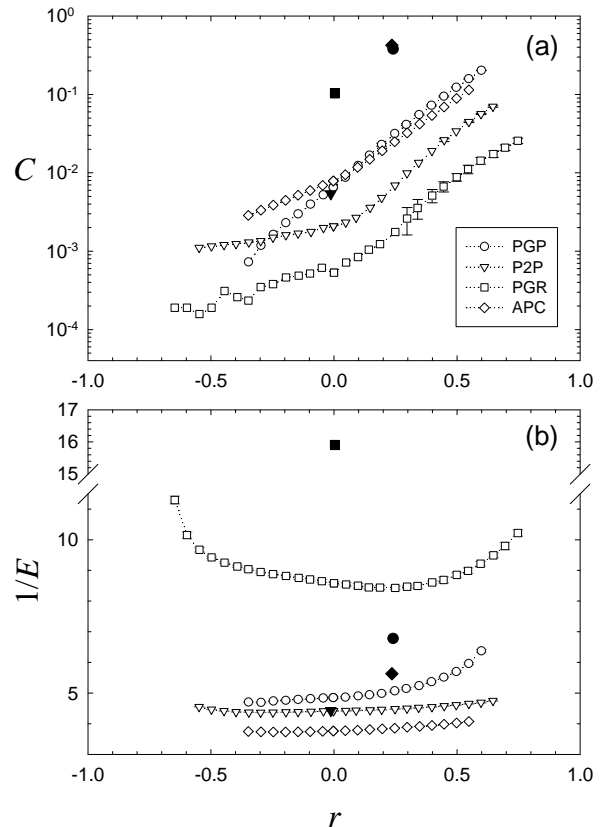


FIG. 9:  $C$  and  $1/E$  vs  $r$ , for real networks. Original values, before rewiring, are also indicated (filled symbols). PGP (Pretty Good Privacy encrypted communication network) [22]:  $N = 10680$ ,  $\langle k \rangle \simeq 4.55$ ; P2P (Gnutella peer-to-peer network) [23]:  $N = 10876$ ,  $\langle k \rangle \simeq 7.35$ ; PGR (power grid) [24],  $N = 4941$ ,  $\langle k \rangle \simeq 2.67$ ; APC (astrophysics collaboration) [25]:  $N = 16706$ ,  $\langle k \rangle \simeq 14.5$ .

other than the tails. These deviations can be attributed to different initial power law regimes. (iv) Finally, APC has a power-law decay with exponent  $\gamma \simeq 1$  and exponential cut-off for  $k > 50$  [25]. The low and constant plot of  $1/E$  vs  $r$  is expected for a network with large  $\langle k \rangle$ , almost independently of the class of degree distribution. The large values of  $C$  are also consistent with heterogeneous distributions with large  $\langle k \rangle$ .

Then, despite the different details of real degree distributions, the main observed features can be interpreted in terms of the analyzed classes with corresponding values of parameters  $\langle k \rangle$  and  $N$ .

#### IV. DISCUSSION AND FINAL REMARKS

For all classes of networks considered,  $C$  increases with  $r$  in the whole allowed range of  $r$  (see also Ref. [10], where positive values of  $r$  were analyzed). However, we observed that, in the  $r$ -ensemble, a non-vanishing clustering coefficient  $C$  is typically due to finite size effects,

such that, in the large size limit, network transitivity vanishes as  $1/N$ . In contrast, for power-law networks characterized by  $r$  above a threshold, a significantly non-null transitivity arises, apparently persisting for large  $N$ .

In any case, since rewiring in the  $r$ -ensemble turns  $C$  typically small, transitivity does not seem to contribute for attaining the prescribed value of  $r$ . To identify the factors that contribute to  $r$ , it is useful to rewrite Eq. (1). Recalling that  $\langle k^n \rangle_e = \langle k^{n+1} \rangle / \langle k \rangle$  [26], where  $\langle \dots \rangle$  (without subindex) means computed over the degree distribution  $P(k)$ , then Eq. (1) becomes

$$r = \frac{\langle k \rangle^2 \langle k k' \rangle_e - \langle k^2 \rangle^2}{\langle k \rangle \langle k^3 \rangle - \langle k^2 \rangle^2}. \quad (8)$$

Following the decomposition made by Estrada [12], notice that the quantity  $\tilde{P}_3 \equiv \sum_{(k,k')} (k-1)(k'-1)$ , where the sum is performed over all the different pairs of neighboring vertices, is the number of paths of length three, then  $P_3 = 3n_\Delta + P_3$ , where  $P_3$  is the number of nontriangular paths of length three (involving four vertices). As done in Eq. (5) for  $3n_\Delta$ , let us scale also  $P_3$  by the number of wedges (paths of length two)  $P_2 = \frac{1}{2} \sum_i k_i(k_i - 1)$ , defining  $B = P_3/P_2$  (scaled branching) [12]. Then Eq. (8) can be written as

$$r = \frac{\langle k \rangle (\langle k^2 \rangle - \langle k \rangle) \left( B + 1 - \frac{\langle k^2 \rangle}{\langle k \rangle} + C \right)}{\langle k \rangle \langle k^3 \rangle - \langle k^2 \rangle^2}. \quad (9)$$

Expression (9) is determined by the three first raw moments of  $P(k)$ , and also by  $B$  and  $C$  that are the quantities embodying the information on the linear degree-degree correlations.

For the Poisson distributed networks, by taking into account the analytical expressions for the moments of  $P(k)$ , it is straightforward to see that

$$r = B - \langle k \rangle + C. \quad (10)$$

Clearly, disassortative correlations are favored by vanishing  $C$ . Only for positive  $r$  the growth of  $C$  is convenient, but  $B - \langle k \rangle$  can vary in a wider interval than  $C$  (twice wider in this case). The existence of two regimes in the increase of  $C(r)$ , observed in Fig. 2, is consistent with this picture. In other words, Eq. (10) indicates that, in the rewiring process of a Poisson network to attain  $r_*$ , as soon as  $P(k)$  is conserved and  $C$  remains very small, then  $r$  is ruled predominantly by  $B$ .

For the power-law distributed networks, some qualitatively similar effects occur, as far as the relation of  $r$  with  $B$  and  $C$  is always linear and  $C$  is constrained to a narrower interval than  $B$ . The formation of triangles also in this case contributes only for assortative values of  $r$

(above the crossover), with values of  $C$  larger than in the Poisson case but still small. Then also in this case the increase of the branching must drive rewiring. In contrast to the Poisson case, the other terms in Eq. (9), related to the moments of  $P(k)$ , might have a crucial influence on  $r$  because of the divergence, in the infinite network limit, of the  $n$ th moments for  $\gamma \geq n + 1$ .

Let us analyze the large  $k_{max}$  (hence  $N$ ) limit, setting aside the marginal (logarithmic) cases. Considering the expressions for the moments (e.g., Eq. (6)), one has, for  $3 < \gamma < 4$ :  $r \sim [B - \mathcal{O}(1)] / \mathcal{O}(k_{max}^{4-\gamma})$ , while for  $2 < \gamma < 3$ :  $r \sim [B - \mathcal{O}(k_{max}^{3-\gamma})] / \mathcal{O}(k_{max})$ , meaning  $\mathcal{O}(x^\alpha) \sim ax^\alpha$ , with  $a > 0$ . To approach the lower limit  $r = -1$ , one must have minimal  $B$ . If it is of order greater than the other terms in the numerator, then one can not have negative  $r$ , because  $B$  is non-negative and it will dominate the numerator. Thus, negative  $r$  can arise only if  $B$  is of the same or lower order. But in that case  $r \rightarrow 0$  in the large  $k_{max}$  limit. This explains why the lower bound  $r_{min}$  tends to 0 when  $\gamma \leq 4$  (see Fig. 3(b)). Along this line, however,  $r_{min}$  is not expected to vanish when  $\gamma > 4$ , but to tend to a small finite value. Similarly, to attain a non-null upper bound of  $r$ ,  $B$  needs to grow like the denominator, otherwise, the upper bound will be negative and also vanish when  $k_{max} \rightarrow \infty$ , leading to the collapse of the upper bound too. However, this does not necessarily happens if  $B$  is driven to grow enough during rewiring, which is what seems to be happen according to Fig. 3(b).

The connection between  $r$  and distance measures is no so direct analytically. Numerical results showed that, for networks with localized distribution of links, changing  $r$  modifies significantly the mean path length only when correlations are assortative ( $r > 0.5$ ) and  $\langle k \rangle$  small. These changes are related to the induced fragmentation, that diminishes by increasing  $\langle k \rangle$ . Then, the impact of  $r$  becomes less important as  $\langle k \rangle$  increases. Meanwhile, the influence on the diameter is more dramatic. In power-law networks, the modification of the mean path length by  $r$  is a bit more marked even if fragmentation is absent for  $\langle k \rangle \geq 4$ , while the diameter is not largely affected. In both cases, the modification of characteristic lengths that occur when varying  $r$  may affect transport processes and should be taken into account either when interpreting or designing numerical experiments on top of these networks.

### Acknowledgements:

We acknowledge partial financial support from CNPq and FAPERJ (Brazilian Government Agencies).

- Phys. Rev. E **77**, 066112 (2008); R. Cohen and S. Havlin, Phys. Rev. Lett. **90**, 058701 (2003).
- [3] Y. Xue, J. Wang, L. Li, D. He and B. Hu, Phys. Rev. E **81**, 037101 (2010).
- [4] Y. Moreno, J.B. Gómez, A.F. Pacheco, Phys. Rev. E **68**, 035103(R) (2003).
- [5] M. Boguñá, R. Pastor-Satorras, Phys. Rev. E **66**, 047104 (2002).
- [6] J. Menche, A. Valleriani, R. Lipowsky, Phys. Rev. E **81**, 046103 (2010).
- [7] M. E. J. Newman, Phys. Rev. E **67**, 026126 (2003).
- [8] R. Xulvi-Brunet, I. M. Sokolov, Phys. Rev. E **70**, 066102 (2004).
- [9] J. Park, M. E. J. Newman, Phys. Rev. E **70**, 66117 (2004).
- [10] D. V. Foster, J. G. Foster, P. Grassberger, M. Paczuski, Phys. Rev. E **84**, 066117 (2011).
- [11] J.D. Noh, Phys. Rev. E **76**, 026116 (2007).
- [12] E. Estrada, Phys. Rev. E **84**, 047101 (2011).
- [13] M.E.J. Newman, PNAS **98** (2), 404 (2001).
- [14] S. Boccaletti, V. Latora, Y. Moreno, M. Chavez, D.-U. Hwang, Phys. Repts. **424**, 175 (2006); V. Latora and M. Marchiori, Phys. Rev. Lett. **87**, 198701 (2001).
- [15] P. Erdős and A. Rényi, Publ. Math. Debrecen **6**, 290 (1959); R. Albert, A. L. Barabási, Rev. Mod. Phys. **74**, 47 (2001).
- [16] M. Molloy and B. Reed, Random Structures & Algorithms **6** 161 (1995); M.E.J. Newman, *Networks: An Introduction* (Oxford University Press, Inc., New York, NY, USA, 2010).
- [17] L. Gallos, Phys. Rev. E **70**, 046116 (2004).
- [18] S. M. Ross, *Simulation* (Academic Press, 2006); M. E. J. Newman, G. T. Barkema, *Monte Carlo Methods in Statistical Physics* (Oxford University Press, USA, 1999).
- [19] S. Maslov, K. Sneppen, Science **296**, 910 (2002).
- [20] S. N. Dorogovtsev, J. F. F. Mendes and A. N. Samukhin, Phys. Rev. Lett. **85**, 4633 (2000).
- [21] D. J. Watts and S. H. Strogatz, Nature (London) **393**, 440 (1998).
- [22] M. Boguñá, R. Pastor-Satorras, A. Díaz-Guilera, A. Arenas, Phys. Rev. E **70**, 056122 (2004).
- [23] Data can be found at <http://snap.stanford.edu/data/p2p-Gnutella04.html>
- [24] D. J. Watts, S. H. Strogatz, Nature **393**, 440 (1998); data can be found at <http://www-personal.umich.edu/~mejn/netdata/>
- [25] M. E. J. Newman, Proc. Natl. Acad. Sci. USA **98**, 404 (2001); Data at <http://www-personal.umich.edu/~mejn/netdata/>
- [26] S.N. Dorogovtsev, A.L. Ferreira, A. V. Goltsev, J. F. F. Mendes, Phys. Rev. E **81**, 031135 (2010).